International Journal of Energy Engineering 2020, 10(1): 1-9
DOI: 10.5923/j.ijee.20201001.01

Latent Heat Storage During Melting and Solidification of a Phase Change Material (PCM) Embedded with a Porous Matrix of High Thermal Conductivity

Mehdi Fteiti[1,*], Amel Alaidrous[2]

[1]Collegue of Preparatory Year, Umm Al Qura University, Makkah Al Mukarramah, Saudi Arabia
[2]Department Mathematical Sciences, Umm Al Qura University, Makkah Al Mukarramah, Saudi Arabia

Abstract The objective of the present work is to analyse numerically the effect of embedding a porous matrix (PMX) of high thermal conductivity within a phase change material (PCM) on the heat energy storage and recovery during the melting and solidification of a PCM. Most of the previous work put the insight mainly on the charging process during melting. The present study focuses on both charging and discharging during melting and solidification. Constant heat flux is applied through the left wall of a rectangular storage unit. The other walls are kept thermally insulated. At the end of the heating period, a cooling stage starts to extract the heat through the same wall. The ratio of thermal conductivities $\lambda_{PMX}/\lambda_{PCM}$ of the porous matrix and the PCM will be taken as a parameter to study the efficiency of the thermal storage. Results are presented in terms of temperature fields, liquid-solid interface progress and plots of latent, and sensible heat storage. The study shows that a significant improvement in the heat storage/recovery can be achieved. For better efficiency, a compromise should be established between the ratio of thermal conductivity and the heating period.

Keywords Latent heat storage, Thermal conductivity enhancement, Phase change material, Porous media, Natural convection

1. Introduction

Thermal energy storage TES is a promising alternative for bridging the gap between energy demand and supply during peak periods. Solar radiation, which is an exhaustible clean and renewable source of heat, and heat wasting in industrial processes, can be used as buffering systems. Thermal energy is easily storable by raising the temperature of a storage medium (sensible heat storage SHS) or changing its state (latent heat storage LHS). But, Latent heat storage during melting and solidification is much more attractive because of its high storage capacity. Another advantage, LHS occurs in a small range of temperatures and requires much lower volume. Phase change materials have shown great potential in thermal storage applications. Providing new PCMs with a variety of characteristics is now an attractive field of research. Agyenim & *al.* [1] presented an overview of different PCMs and their applications in thermal storage systems, operating at low temperatures (below 60 ℃) suitable for domestic heat storage applications. Different configurations of storage units studied numerically and experimentally are quoted in this paper. A survey on storage materials operating at high temperature (between 120 ℃ and 1000 ℃) used for industrial applications, was reported by Murat [2]. Recently, Yaxue *& al.* [3] reviewed the state of the art of PCMs and their applications, where a deep insight was attached to the development of new materials of better storage performance. The major drawback of such PCMs is related to their low thermal conductivity which limits the charge and discharge rates during melting and solidification. Thermal conductivity enhancement (TCE) is crucial to improve the efficiency of LHS systems. During the last decades, different methods of TCE have been proposed to overcome the large thermal resistance of the PCMs, a recent review was given by Liwu *& al.* [4]. TCE techniques are mainly based on two strategies: The first, consists of the incorporation within the PCM of dispersed high thermal conductivity particles with variable volume proportions [5]. The size of these particles varies from Nano-scales [6] to micro scales [7]. The second strategy is based on the inclusion of different types of fixed structures such as fins, heat pipes, metal foam, strips, and ships. The inclusion of fins is a systematic option inspired from the heat exchangers design and consists of the extension of the surface area between the PCM and the heated fluid [8-9] Sciacolvelli &

* Corresponding author:
mafteiti@uqu.edu.sa (Mehdi Fteiti)
Published online at http://journal.sapub.org/ijee

al. [10] apply Y-shaped fins with different lengths and angle spacing in a shell-and-tube LHS unit and showed that TES may be improved by 24%. Al-Abidi *& al.* [11] investigated the efficiency of LHS inside a triplex tube experimentally and showed that the charging time is significantly reduced with the application of internal and external fins. The use of heat pipes can be found in [12-13]. Sharifi *& al*. [14] investigated experimentally and computationally the melting and solidification of PCM surrounding a vertical heat pipe, finned with metal foils in a vertical cylinder. The combination of HP-metal foils shows a better increase of the phase change rates than the use of only one of them. Encapsulation and micro encapsulations of PCMs have been used as TCE techniques both in energy storage and energy building applications [15-16]. The inclusion of a porous matrix as a fixed structure, which is the subject of the present work, was among the earliest TCE techniques. It is easier to consider irregular fixed inclusions like porous structures. Tong & *al.* [17] studied the enhancement of thermal conductivity numerically by inserting an aluminium matrix in a cylindrical annulus saturated with a water/ice mixture. The study includes the effects of diffusion and natural convection during both melting and solidification, and the Darcy equation was applied for modelling the fluid flow. Results show a marked heat transfer enhancement for small volume fractions, but for further increase of the volume fraction, the enhancement rate does not increase linearly. Xavier & *al.* [18] considered a porous graphite matrix, a concentrated expanded natural graphite (CENG) to study the solidification of a paraffin/CENG composite. The thermal conductivity was improved from (0.24 K m^{-1} W^{-1}) for pure paraffin to a range between (4 to 70 K m^{-1} W^{-1}) depending on the graphite bulk density. The overall solidification time was reduced; nevertheless, an optimization was proposed due to the antagonist behaviours of the thermal power and thermal capacity according to the paraffin/CENG composition. Mesalhy & *al.* [19] studied, numerically, the melting between two concentric cylinders of a PCM inside a porous matrix of high thermal conductivity. The inner cylinder is heated by a temperature higher than the melting temperature of the PCM while the outer cylinder was kept adiabatic. The problem was solved numerically using the two equations model and the Darcy-Brinkman-Forchiemer formulation. Zhenyu & *al.* [20] investigated a shell-and-tube LHS unit holding a PCM embedded with a metal foam matrix. The numerical modelling took into account the natural convection and was solved using the enthalpy porosity formulation. They pointed out that heat transfer can be enhanced by more than seven times. Taeil & *al.* [21] analysed a latent heat thermal energy storage system (LHTES) for concentrated solar power consisting of a tank filled with tubes carrying heat transfer fluid, by using a PCM/Graphite foam composite, the number of tubes is dramatically reduced compared with the case of PCM without Graphite foam. Also, Zhuo & *al.* [22] investigated the melting of Sodium Nitrate ($NaNO_3$) inside a metal skeleton of Copper where they numerically analysed the effects of heat conduction through the metal structure and natural convection in the liquid PCM. They also studied detailed parameters such as porosity and pore density of the metal matrix on the TES systems, in both melting and solidification processes. In recent work, Sayed & *al.* [23] studied the performance of a LHTES system made of a porous structure filled with a nano PCM which is a PCM combined with a volume fraction of a high thermal conductivity nanoparticles. The authors investigated the effect of varying the nanoparticles volume fraction and the natural convection on the melting process, but they did not consider the case of solidification. Their results focus on a comparison between a scale analysis and the numerical model proposed. To analyze the effect of pore distribution, Zilong & *al.* [24] studied the melting of PCM in a porous metal foam characterized by fractal geometry. They found that the dimension of the fractals and their distribution can affect the melting time. Recently, Esapour & *al.* [25] conducted a numerical investigation of the melting and solidification of a PCM embedded in a porous metal foam in a multi-tube heat exchanger. A recent numerical investigation has been conducted by Jourabian & *al*. [26] concerning the melting of a PCM in a porous media around two hot cylinders using the lattice Boltzmann method. Most of the previous works show that the enhancement of the thermal conductivity of the porous medium contributes to the increase of the storage performance of LHTES systems. The present study focuses on both the melting and solidification of the PCM and the effect of the thermal conductivity ratio on the performance of the energy storage/recovery processes. Furthermore, the study illustrates the relationship between the heating period and the thermal conductivity ratio and their effect on the sensible and the latent heat storage.

2. Problem Definition and Modelling

Consider a two-dimensional rectangular domain of width L and height H (Fig.1), filled with a porous structure (solid matrix) and saturated with a PCM. Initially, the solid matrix and the PCM are supposed to be in thermal equilibrium at the melting temperature of the PCM. A constant and uniform heat flux Q will be applied on the left vertical wall of the cavity, while the remaining walls are kept insulated. The mathematical formulation of the problem is based on the volume averaging approach [27]. The Darcy-Brinkman model and the enthalpy-porosity formulation [28] have been adopted to describe the flow in porous media with one energy equation for the whole domain. The following approximations have been considered:

- Thermo-physical properties are assumed to be constant in both liquid and solid phases, except for the density which is supposed to obey the Boussinesq assumption in order to take into account the natural convection.
- The fluid in the liquid phase is assumed to be newtonian and the flow is unsteady and laminar.
- Viscous dissipation is negligible.

- Thermal equilibrium condition is adopted between the PCM and the porous structure.
- No-slip boundary conditions for the velocities at the walls are implemented.

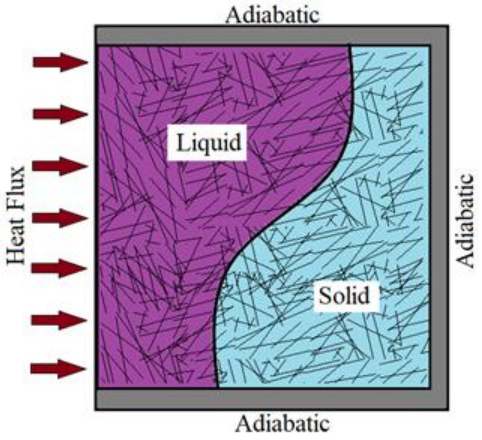

Figure 1. Physical domain

The governing equations describing the problem are:
Mass conservation equation:

$$\frac{\partial u}{\partial x}+\frac{\partial v}{\partial y}=0 \tag{1}$$

x-Momentum equation:

$$\frac{1}{\varepsilon}\frac{\partial u}{\partial t}+\frac{1}{\varepsilon^2}\left(u\frac{\partial u}{\partial x}+v\frac{\partial u}{\partial y}\right) = -\frac{1}{\rho}\frac{\partial p}{\partial x}+\frac{\nu}{\varepsilon}\left(\frac{\partial^2 u}{\partial x^2}+\frac{\partial^2 u}{\partial y^2}\right)-\frac{\nu}{K}u+C_k u \tag{2}$$

y-Momentum equation:

$$\frac{1}{\varepsilon}\frac{\partial v}{\partial t}+\frac{1}{\varepsilon^2}\left(u\frac{\partial v}{\partial x}+v\frac{\partial v}{\partial y}\right)=-\frac{1}{\rho}\frac{\partial p}{\partial y}+\frac{\nu}{\varepsilon}\left(\frac{\partial^2 v}{\partial x^2}+\frac{\partial^2 v}{\partial y^2}\right)-\frac{\nu}{K}v +C_k v+\rho g\beta_T\left(T-T_{ref}\right) \tag{3}$$

Conservation of energy:

$$(\rho C_p)^*\frac{\partial T}{\partial t}+(\rho C_p)_l\left(u\frac{\partial T}{\partial x}+v\frac{\partial T}{\partial y}\right) = \lambda_{eff}\left(\frac{\partial^2 T}{\partial x^2}+\frac{\partial^2 T}{\partial y^2}\right)-L_H\frac{\partial f_l}{\partial t} \tag{4}$$

Where, ε is the porosity of the domain, K the permeability of the porous medium, λ_{eff} is the effective thermal conductivity of the PCM/PMX medium, β_T is the thermal expansion of the liquid PCM, and f_l is the local liquid fraction of the melted PCM.

The effective heat capacity and the effective thermal conductivity are calculated in terms of the porosity as follows:

$$(\rho C_p)^*=\varepsilon\left[f_l(\rho C_p)_{PCM_l}+(1-f_l)(\rho C_p)_{PCM_s}\right] +(1-\varepsilon)(\rho C_p)_{PMX}$$

$$\lambda_{eff}=\varepsilon\left[f_l\lambda_{PCM_l}+(1-f_l)\lambda_{PCM_s}\right]+(1-\varepsilon)\lambda_{PMX} \tag{6}$$

The following dimensionless variables are introduced: $X=\frac{x}{H}, Y=\frac{y}{H}$, $F_o=\frac{\alpha t}{H^2}$, $U=\frac{uH}{\alpha}$, $V=\frac{vH}{\alpha}$, $P=\frac{pH^2}{\alpha^2\rho}$ and $\theta=\frac{T-T_m}{\Delta T}$. Where $\Delta T=\frac{Q_o H}{\lambda_{PCM}}$ and Q_o is a reference heat flux.

In dimensionless form the following equations are obtained:

$$\frac{\partial U}{\partial X}+\frac{\partial V}{\partial Y}=0 \tag{7}$$

$$\frac{1}{\varepsilon}\frac{\partial U}{\partial F_o}+\frac{1}{\varepsilon^2}\left(U\frac{\partial U}{\partial X}+V\frac{\partial U}{\partial Y}\right) = -\frac{\partial P}{\partial X}+\frac{P_r}{\varepsilon}\left(\frac{\partial^2 U}{\partial X^2}+\frac{\partial^2 U}{\partial Y^2}\right)-\frac{P_r}{D_a}U+C_k U \tag{8}$$

$$\frac{1}{\varepsilon}\frac{\partial V}{\partial F_o}+\frac{1}{\varepsilon^2}\left(U\frac{\partial V}{\partial X}+V\frac{\partial V}{\partial Y}\right)=-\frac{\partial P}{\partial Y}+\frac{P_r}{\varepsilon}\left(\frac{\partial^2 V}{\partial X^2}+\frac{\partial^2 V}{\partial Y^2}\right)-\frac{P_r}{D_a}V +C_k V+R_a.P_r.\theta \tag{9}$$

$$\sigma_1\frac{\partial\theta}{\partial F_o}+U\frac{\partial\theta}{\partial X}+V\frac{\partial\theta}{\partial Y}=\sigma_2\left(\frac{\partial^2\theta}{\partial X^2}+\frac{\partial^2\theta}{\partial Y^2}\right)-\frac{1}{Ste}\frac{\partial f_l}{\partial F_o} \tag{10}$$

Where:

$$\sigma_1=\varepsilon+(1-\varepsilon)\left(\rho C_p\right)_{PMX}/\left(\rho C_p\right)_{PCM}$$

$$\sigma_2=\varepsilon[f_l+(1-f_l)\chi]+(1-\varepsilon)\chi,\ \chi=\lambda_{PMX}/\lambda_{\mathrm{PCM}}$$

χ is a parameter that represents the ratio between the thermal conductivity of the porous matrix and the PCM.

The dimensionless parameters in the equations (7)-(9) are defined in the nomenclature. These parameters are the Rayleigh number Ra, the Prandtl number Pr, the Stefan number Ste and the Darcy number Da.

Boundary conditions:

$$\left.\begin{array}{l} Q=+1\ Heating\ condition \\ Q=-1\ Cooling\ condition \end{array}\right\}\ at\ X=0,$$

$$dQ/d\mathrm{x}=0\ at\ \mathrm{X}=0.5$$

$$dQ/d\mathrm{y}=0\ at\ \mathrm{Y}=0$$

$$dQ/d\mathrm{y}=0\ at\ Y=1$$

3. Numerical Validation

The numerical method used to solve the governing equations (7-10) is the control-volume finite element method CVFEM. This method was historically introduced by Baliga & Patankar [29] for handling convection-diffusion problems. The discretization by the CVFEM allows to take six neighbouring points around each central point of the domain. The obtained discretised equation can be written in the following form:

$$a_P\phi_P=\sum_{n=1}^{6}a_{nb}\phi_{nb}+b \tag{11}$$

Where ϕ is a general variable that can be $u, v\ or\ T$. The total implicit scheme was used for the time discretization and the SIMPLER algorithm for the pressure-velocity coupling. The resulting algebraic system was solved by the TDMA line by line solver. The term C_k in the source terms of the momentum equations (8) and (9) corresponds to the enthalpy-porosity formulation defined by Brent *& al.* [28]:

$$\mathrm{C_k}=-\mathrm{C_m}\left(\frac{1-f_l^2}{f_l^3+b}\right)$$

Where f_l is the liquid fraction, C_m is a parameter depending on the morphology of the porous medium and is taken equal to 10^6; $b=0.001$ is introduced to avoid division by zero. To track the phase change front during the melting or the solidification, the update of the liquid fraction is determined by the following approach:

$$f_l^{n+1} = f_l^n + \omega \frac{Ste \times \Delta F_0}{A_V} a_p(\theta_p - \theta_m)$$

Where A_V is the area of the control volume, and ω is an under relaxation coefficient. The numerical method was first tested for the case of natural convection in a square enclosure, filled with a porous medium saturated with air, without considering the phase change. The vertical walls of the enclosure are subject to a horizontal temperature gradient while the bottom and the top walls are thermally insulated. The obtained results are presented in Table 1, in terms of average Nusselt number. Comparison with the numerical results obtained by Bennacer *& al.* [30] and Lauriat *& al.* [31] shows a good agreement. A second validation was performed to examine the capabilities of the numerical method to handle phase change problems. The numerical test consists of the melting of a pure metal (Gallium) in a square cavity of width $L=8.89$ *cm* and height $H=0.635$ *cm*. The left side of the cavity is subject to a hot temperature $T_H=38$ ℃ and the right wall is subject to a constant temperature *1* ℃ below the melting temperature of the gallium $T_m=28$ ℃ attempting to minimize subcooling effects. The horizontal walls are maintained adiabatic.

Table 1. Average Nusselt number, natural convection in porous medium ($A=1$, $Pr=0.71$) Darcy- Brinkman model. $\boldsymbol{R_a^*}=Ra.Da$

		Da				
	$\boldsymbol{R_a^*}$	$\mathbf{10^{-6}}$	$\mathbf{10^{-5}}$	$\mathbf{10^{-4}}$	$\mathbf{10^{-3}}$	$\mathbf{10^{-2}}$
Present work	500	8.72	8.42	7.33	5.42	3.30
Lauriat et al.[31]		8.72	8.41	7.35	5.42	3.30
Bennacer et al.[30]		8.68	8.37	7.30	5.38	3.26
Present work	10^3	-	12.45	-	-	4.26
Lauriat et al.[31]		-	12.42	-	-	4.26
Bennacer et al.[30]		-	12.26	-	-	4.18

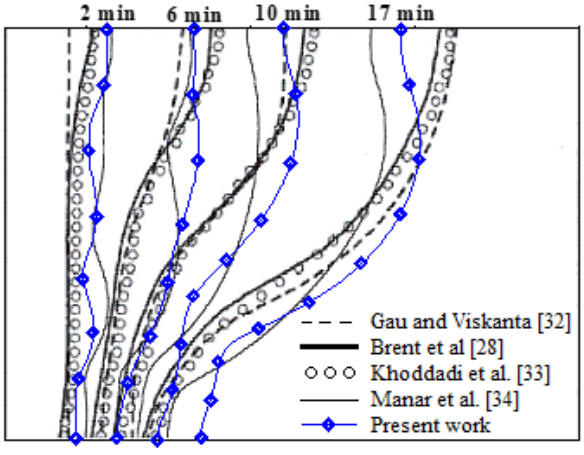

Figure 2. Interface location at different times

The dimensionless parameters for this problem are Ra=6.5x10^5, Pr=0.0216 and Ste=0.039. The obtained results are presented in Fig.2, where plots of the interface location at different times are compared to the experimental results of Viskanta *& al.* [32] and also to other different numerical results [28,33,34]. It can be shown that the results are acceptable even though some discrepancies are noticed between the numerical results due to the use of different numerical schemas.

Grid and time step independencies are tested for the grid sizes 41x81 and 61x121 and for dimensionless time steps 2x10^{-5} and 10^{-4}. Results in terms of isotherms at the dimensionless time τ=0.04 and the melting front at τ=0.06 are represented in Fig. 3. The rest of simulations will be executed for a grid size 41x81 and a time step 2x10^{-5}.

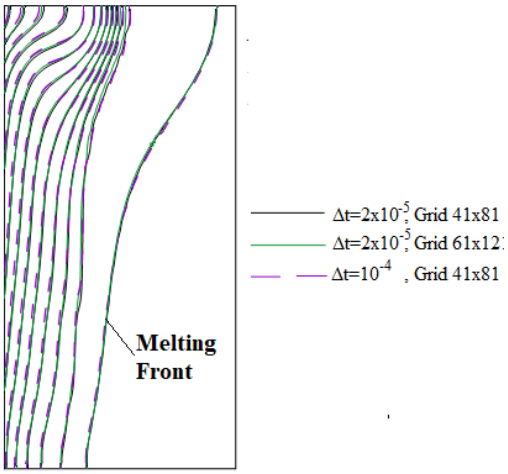

Figure 3. Isotherms at the dimensionless time τ=0.04 and the Melting front *at* τ=0.06

4. Numerical Results and Discussion

4.1. Effect of Thermal Conductivity Enhancement

The problem of melting inside a rectangular cavity heated by constant temperature on one vertical side and cooled on the opposite side has been extensively studied. In the present study, we consider the case where the cavity is heated by a uniform heat flux on one vertical side, while the opposite side is adiabatic. In addition, the study includes both melting and solidification inside a porous structure. The cavity is first subjected to a positive heat flux during a heating period τ_H. At the end of this period, a cooling stage starts, during which latent heat is extracted by solidification. To examine the effect of thermal conductivity enhancement, a simulation was first performed for a PCM-alone (n-octadecane) and then for a PCM embedded within a porous structure (Expanded Graphite). Thermophysical properties of n-octadecane and expanded graphite are listed in Table 2. Several dimensionless parameters govern the problem: the Rayleigh number *Ra*, the Prandtl number *Pr*, the Stefan number *Ste*, the porosity ε and the Darcy number *Da*. The parameter on which we focus in the present study is the ratio between the thermal conductivity of the material structure

and the PCM ($\chi = \lambda_{PMX}/\lambda_{PCM_l}$). To ensure that the condition of thermal equilibrium between the solid matrix and the PCM will be satisfied, so a model of one equation can be used, intermediate values of χ have been considered ($\chi \approx 10^2$). The dimensionless time was taken as the product of the Fourier and the Stefan numbers, $\tau = F_o \times Ste$ which is a characteristic parameter for the time in the solid-liquid phase change problems.

Table 2. Thermophysical properties of PCM (n-Octadecane) and Expanded graphite [36]

Variable	PCM_l	PCM_s	Graphite
Conductivity λ (W/mK)	0.358	0.148	12
Specific heat C_p (J/kg K)	2153	2153	830
Density ρ (kg/m^3)	814	779	1300
Latent heat of fusion L_H (kJ/kg)	206.8		
Melting temperature T_m (℃)	26.95		

The parameters used for the comparison between the storage in pure PCM (n-octadecane) and PCM embedded with the expanded graphite matrix (PCM-EGR) are Ra=2x10^6, Pr=50, Ste=0.1, A=2, ε=0.95 and χ=88.

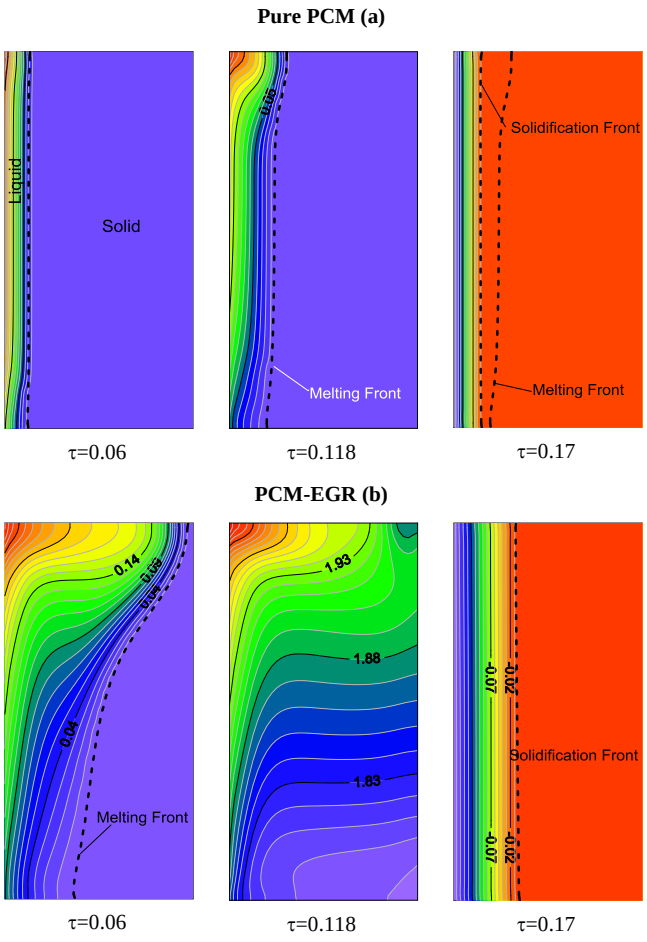

Figure 4. Temperature contours and liquid-solid front for pure PCM (a) and PCM-EGR mixture (b)

Fig. 4 shows the temperature contours and the liquid-solid interface location during the melting and the solidification stages for both cases of pure PCM and PCM-EGR. It is clear from this figure that, the melting and the solidification rates are enhanced with the inclusion of the thermal conductivity enhancer. This is manifestly due to the improvement of the heat transfer compared to the case of pure PCM. Hence, at the dimensionless time τ =0.06, for the PCM-EGR mixture, the shape of the isotherms shows that the melting is dominated by natural convection, also the liquid-solid front is more in advance compared to the case of pure PCM. At this same instant for the pure PCM, conduction heat transfer is still dominant, the isotherm lines are parallel and the liquid fraction thickness shows that the melting is progressed with a lower rate. At the dimensionless time τ=0.118, just before the end of the heating time (τ_H=0.12), for the PCM-EGR, the disappearance of the liquid-solid front and the shape of the isotherm lines indicate that the PCM is wholly turned into liquid. The acceleration of melting is then clearly apparent with the inclusion of the porous matrix. The isotherm values show also an increase of temperature of the storage medium which means that the melted domain is superheated. While for the pure PCM, the melting front is still at its early stage (Fig. 4-a).

After applying the cooling condition, at τ=0.17, a solid layer starts to grow along the left vertical wall. The latent heat recovery begins with the onset of solidification. The rate of recovery is as high as the speed of solidification. Although solidification starts earlier for the pure PCM, it is becoming more advanced for PCM-EGR mixture. This is the result of the increase of the thermal conductivity with the inclusion of the porous matrix. Fig. 4 -a shows that for the pure PCM besides the solidification front, the melting front is still apparent because the fusion was not entirely completed.

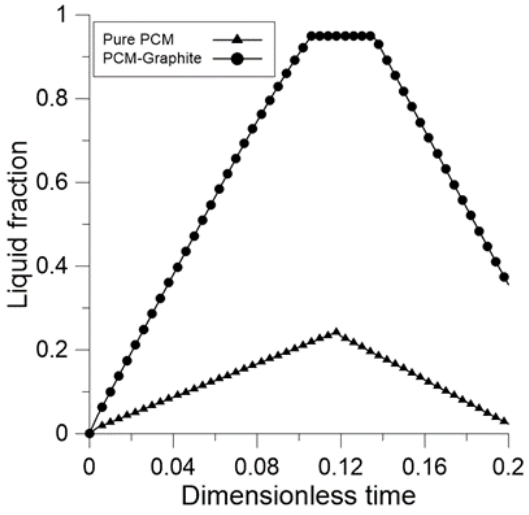

Figure 5. Liquid fraction during melting and solidification

Fig. 5 illustrates the time evolution of the liquid fraction during the heating and the cooling periods, with and without the embedded solid matrix. The figure shows that the inclusion of the PMX increases the melting and solidification rates. For the pure PCM, at the end of the heating period, the liquid fraction reaches only 25% of its maximum value and begins to decrease immediately after the application of the

cooling condition. However, for the PCM-EGR composite, a full melting is obtained before the end of the heating stage, the liquid fraction attains its maximum value (f_l=1) and a steady-state is obtained (the graph shows a plateau). The rate of melting is increased by 400%. The latent heat stored during the phase change attains its maximum capacity when the PCM is completely melted. If the heating is extended beyond the full melting time, the excess of heat is stored in a sensible form. The temperature of the medium is then increased. As a consequence, when the cooling condition is applied, the solidification process doesn't start immediately. The temperature of medium has to be decreased to the solidification point. During this time the sensible heat is extracted and the latent heat recovery which is more important is delayed. This can be illustrated by the observation of the plateau in the liquid fraction plot (Fig. 5). The extraction of latent heat starts when the liquid fraction stats to decrease. Hence, it can be clearly seen that the inclusion of a high thermal conductivity matrix contributes significantly to the enhancement of the melting and solidification rates, and then the rates of latent heat storage and recovery. Nevertheless, it is worth mentioning that a compromise should be established between the heating period and the thermal conductivity enhancement to promote latent heat storage against sensible heat storage as it will examined in a subsequent section. For more analysis of the effect of thermal conductivity on the melting and solidification of the PCM embedded with the porous structure, four cases have been performed for different values of the thermal conductivity ratio (χ=25, 50, 75 and 100) and a dimensionless heating time (τ_H=0.12).

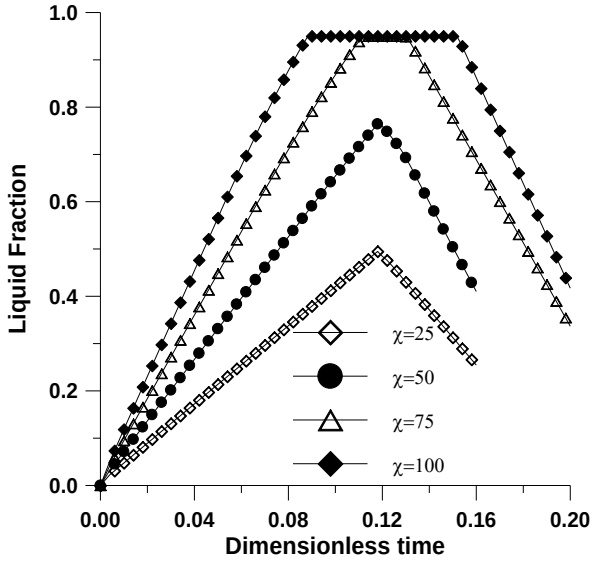

Figure 6. Liquid fraction versus time. Effect of the thermal conductivity ratio. Ra=2x10^6, Pr=50, Ste=0.1, ε=0.95 and Da=10^{-2}

The obtained results are presented in terms of time evolution of the liquid fraction (Fig. 6) as function of χ. The graph shows clearly that the increase of thermal conductivity of the PMX speeds up the melting of the PCM (then the latent storage rate). The same finding is shown for the solidification process (then for the energy recovery rate).

Time evolution of the latent and the sensible heat storage as function of χ are given in Fig. 7 and Fig. 8 respectively. Fig. 7 shows that the latent heat storage rate and capacity are increased with the increase thermal conductivity ratio. Also, the latent heat recovery is faster during the extraction time. Nevertheless, for higher values of χ the melting is faster and then the amount of sensible heat storage during the post melting period is more important as shown in Fig. 8. This effect is not beneficial for the latent energy recovery as it causes the delay of the solidification process. Then for a better optimization and efficiency of the charging/discharging processes the value of χ should be compatible with the heating time to limit the sensible heat storage and to opt preferentially for the latent storage.

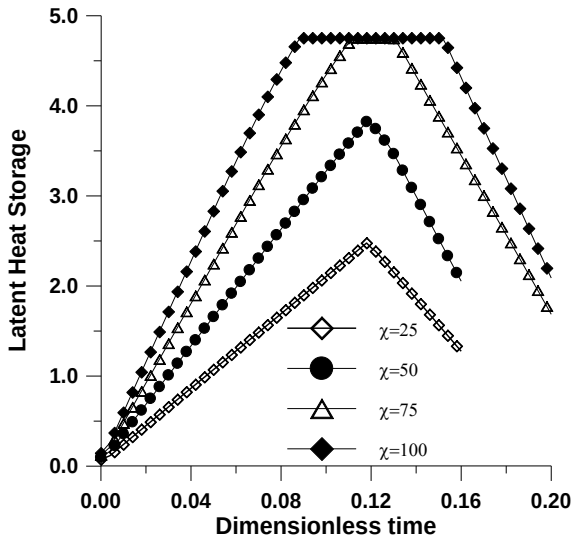

Figure 7. Latent heat versus time. Effect of the thermal conductivity ratio. Ra=2x10^6, Pr=50, Ste=0.1, ε=0.95, χ=75 and Da=10^{-2}

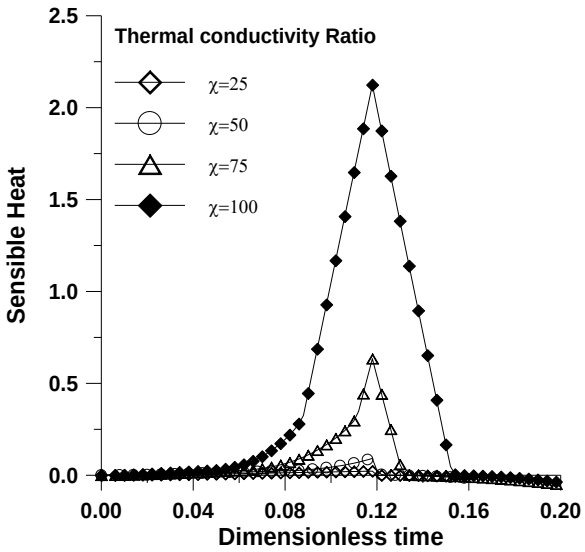

Figure 8. Sensible heat versus time. Effect of the thermal conductivity ratio. Ra=2x10^6, Pr=50, Ste=0.1, ε=0.95, χ=75 and Da=10^{-2}

A simulation of a non-completed melting case is given in Fig. 9, where predictions of the solid and liquid regions are

represented for a heating period τ_H=0.1. It can be shown that at the early stage of heating (τ=0.02), conduction dominates the melting and the liquid front is progressed parallel to the vertical wall. At τ=0.05, the melt width increases, giving rise to the development of natural convection. The natural convection plays a key role by magnifying the heat transfer and then accelerating the melting on the top of the cavity, while at the bottom, conduction is still dominating with smaller heat transfer and slower motion of the interface. As time progresses, the melting front on the top reaches the right wall of the cavity (τ=0.08). At the end of the melting time, a small block of non-melted PCM remains at the bottom right corner. When the left wall starts to be cooled, the solidification front starts to move from left to right. At τ=0.16 the solidification front reaches the melting front, where they are joined in a single front that continues to progress till the material is entirely solidified.

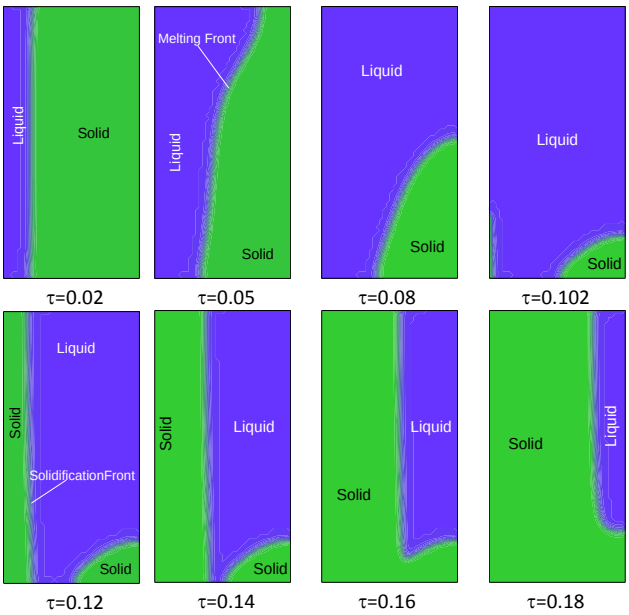

Figure 9. Liquid and solid fractions during the melting and solidification of a PCM-PMX composite. *Ra*=2x10^6, *Pr*=50, *Ste*=0.1, ε=0.95, χ=75 and *Da*=10^{-2}

4.2. Effect of the Heating Time

To examine the effect of the heating period on the energy storage and recovery, the following parameters are maintained constant (*Ra*=2x10^6, *Pr*=50, *Ste*=0.1, ε=0.95, *Da*=10^{-2} and χ=75) and the heating period is modified. Fig. 10 illustrates the latent heat fraction history for the heating periods τ_H=0.1, 0.12 and 0.13. For τ_H=0.1, the latent heat fraction doesn't reach the maximum storage capacity and it starts to decrease immediately after the application of the cooling periods. For the heating periods τ_H=0.12 and τ_H=0.13, complete melting is achieved before the end of the heating time. The plots of the latent heat fraction show a stationary state (plateau) as mentioned earlier. During the stationary state, the absorbed heat is stored inside the medium in sensible form. Fig. 11 shows that the amount of sensible heat increases with the extension of the heating periods. This effect is generally undesirable in the heat storage system because the latent heat is much more important than the sensible heat storage.

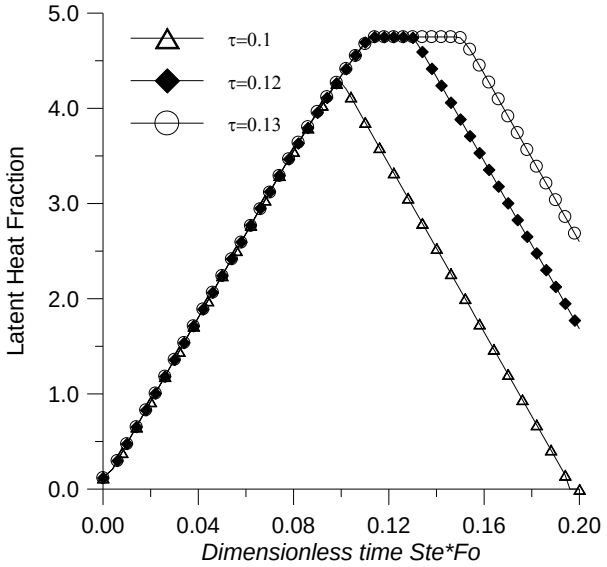

Figure 10. Latent heat storage versus time, effect of the heating period

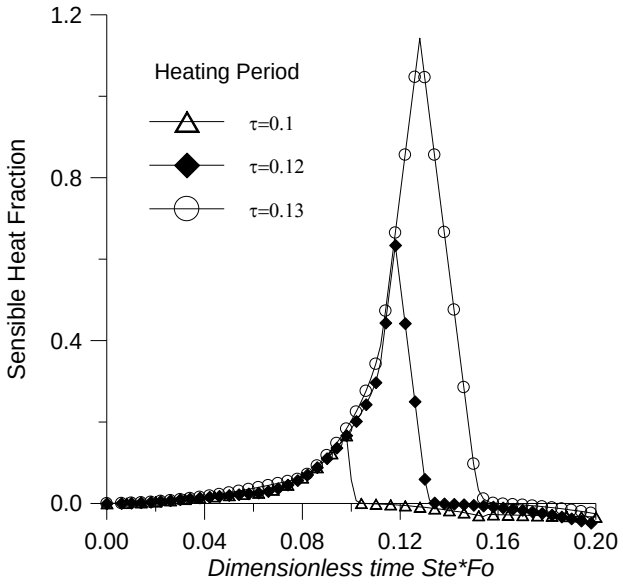

Figure 11. Sensible heat storage versus time. Effect of the heating time

5. Conclusions

This paper presents a numerical investigation of the melting and solidification of a PCM embedded with a porous structure of high thermal conductivity. The enthalpy-porosity formulation and the thermal equilibrium approximation have been adopted in the problem modelling. It was found that the increase of the thermal conductivity contributes to the enhancement of the melting and solidification rates of the PCM and then the heat storage and recovery rates. It was also found that when the heating period exceeds the full melting time, the sensible heat storage will be increased. The growth of sensible heat storage during the

charging period is a drawback because it causes the delay of solidification, then the recovery of latent heat, which is more targeted in heat storage systems because of its higher density.

ACKNOWLEDGEMENTS

Authors are grateful to the King Abdul-Azizi City for Science and Technology (KACST) for supporting this research project.

Nomenclature

English letters

A_v	: Control volume area
a_p	: Discretization coefficient of the central point
Cp	: Specific heat ($J.kg^{-1}.K^{-1}$)
C_k	: Enthalpy-porosity source term
Da	: Darcy number $Da=K/L^2$
Fo	: Fourier Number ($F_o=\alpha t/L^2$)
f_l	: Volume liquid fraction
K	: Permeability (m^2)
L, H	: Length and height of the cavity (m^2)
L_H	: Latent heat of fusion ($J. kg^{-1}$)
Pr	: Prandtl number ($Pr=\nu/\alpha$)
p	: Pressure ($N.m^{-2}$)
P	: Dimensionless Pressure
Ra	: Rayleigh number ($Ra=\rho g\beta L^3/\nu\alpha$)
Ste	: Stefan number ($Ste=C_p\Delta T/L_H$)
T	: Temperature (^oK)
T_{ref}	: Reference temperature ($T_{ref}=T_m$)
t	: Time (s)
u, v	: Velocity components ($m.s^{-1}$)
U, V	: Dimensionless velocity components
Q	: Heat flux
x,y	: Spatial coordinate (m)
X, Y	: Dimensionless space variables

Greek letters

α	: Thermal diffusivity ($m^2.s^{-1}$)
β_T	: Coefficient of thermal expansion (K^{-1})
ε	: Porosity
θ	: Dimensionless temperature
ν	: Kinematic viscosity (m^2s^{-1})
ρ	: Density ($kg\ m^{-3}$)
λ	: Thermal conductivity (W/m K)
λ_{eff}	: Effective thermal conductivity
ω	: Under-relaxation parameter
τ	: Dimensionless time ($\tau=Ste.F_o$)
χ	: Ratio of thermal conductivities ($\chi=\lambda_{PMX}/\lambda_{PCM}$)

Subscripts

l	: Liquid
s	: Solid
m	: melting
PMX	: Porous matrix
PCM	: Phase change material

Abbreviations

TCE	: Thermal conductivity enhancement (or enhancer)
LHS	: Latent heat storage
SHS	: Sensible heat storage
TES	:Thermal energy storage

REFERENCES

[1] F. Agyenim, N. Hewitt, Ph. Eames and. M. Smyth, " A review of materials, heat transfer and phase change problem storage systems (LHTESS)", Renewable and Sustainable Energy Reviews, 14, 615-628, 2010.

[2] Murat M. Kenisarin, "High-temperature phase change materials for thermal energy storage", Renewable and Sustainable Energy Reviews, 14, 955–970, 2010.

[3] L. Yaxue, J. Yuting, G. Alva, G. Fang, "Review on thermal conductivity enhancement, thermal properties and applications of phase change materials in thermal energy storage", Renewable and Sustainable Energy Reviews , 82(3), 32730-2742, 2018.

[4] L. Fan, J.M. Khodadadi, "Thermal conductivity enhancement of phase change materials for thermal energy storage, A review", Renewable and Sustainable Energy Reviews, 15, 24–46, 2011.

[5] S. Jgadheeswarn, S.D Pohekar, "Energy and exergy analysis of particle dispersed latent heat storage system", Int. J of Energy, 1(3), 445-458, 2010.

[6] Min Li, "A nano-graphite/Paraffine phase change material with high thermal conductivity", Applied Energy, 106, 25-35 , 2013.

[7] E. S. Mettawee, G.M.R. Assassa, "Thermal conductivity enhancement in a latent heat storage system", Solar Energy, 81, 839–845, 2007.

[8] M. Gharebaghi, I. Sezai, "Enhancement of heat transfer in latent heat storage modules with internal fins", Numerical Heat Transfer Part A-Appl., 53(7)749-765, 2008.

[9] N. Sharifi, L. Theodore Bergman and A. Faghri, "Enhancement of PCM melting in enclosures with horizontally-finned internal surfaces", Int. J. of Heat and Mass Transfer, 54, 4182-4192, 2011.

[10] F. Sciacovelli, F. Gagliardi and V. Verda, "Maximization of performance of a PCM latent heat storage system with innovative fins", Applied Energy, 707-7015, 2014.

[11] A. Abduljalil Al-Abidi, S. Mat, K. Sopian, M.Y. Sulaiman, A. Th Mohammad, "Experimental study of melting and solidification of PCM in a triplex tube heat exchanger with fins", Energy and Buildings, 68, 33–41, 2014.

[12] H. Shabgard, L.T Bergman, N. Sharifi, A. Fagari, "High temperature latent heat thermal energy storage using Heat pipes", Int. J. Heat and Mass Transfer, 53(15-16) 2979-2988, 2010.

[13] C.W. Robak, Th. L. Bergman, A. Faghri, "Enhancement of latent heat energy storage using embedded heat pipes",

International Journal of Heat and Mass Transfer, 54(15), 3476–3484, 2011.

[14] Nourouddin Sharifi a, Theodore L. Bergman b, Michael J. Allen a, Amir Faghri, Melting and solidification enhancement using a combined heat pipe, foil approach, International Journal of Heat and Mass Transfer, 78, 930–941 (2014).

[15] W. Li, R. Hou, H. Wan, P. Liu, G. He, F. Qin, "A new strategy for enhanced latent heat energy storage with microencapsulated phase change material saturated in metal foam", Solar Energy Materials and Solar Cells, 171, 197–204, 2017.

[16] N. Lakshmi Narasimhan, R. Bharath, Sarah Ann Ramji, M. Tarun, A. Siddarth Arumugam, "Numerical studies on the performance enhancement of an encapsulated thermal storage unit", International Journal of Thermal Sciences, 84, 184-195, 2014.

[17] X. Tong, J.A. Khan, M.R. Amin., "Enhancement of heat transfer by inserting a metal matrix into a phase change material", Numerical Heat Transfer, Part A 30:125–41, 1996.

[18] X. Py, R. Olives, S. Maurin, "Paraffin/Porous-Matrix-Composite as high and constant power thermal energy storage material", International Journal of Heat and Mass Transfer, 44, 2727-2737, 2001.

[19] O. Mesalhy, K. Lafdi, A. Elgafy, K. Bowman, "Numerical study of enhancing the thermal conductivity of a phase change material (PCM) storage using high thermal conductivity porous matrix", Energy Conversion and Management, 46, 847-867, 2005.

[20] Z. Liu, Y. Yao, H. Wu, "Numerical modeling for solid–liquid phase change phenomena in porous media: Shell-and-tube type latent heat thermal energy storage", Applied Energy, 112, 1222–1232, 2013.

[21] T. Kim, D. M. France, W. Yu, W. Zhao, D. Singh, "Heat transfer analysis of a latent heat thermal energy storage system using graphite foam for concentrated solar power", Solar Energy, 103, 438–447, 2014.

[22] Z. Li, Z. Wu, "Numerical study on the thermal behavior of phase change materials (PCMs) embedded in porous metal matrix", Solar Energy, 99, 172–184, 2014.

[23] S. Humaira Tasnim, R. Hossain, S.l Mahmud, A. Dutta, "Convection effect on the melting process of nano-PCM inside porous enclosure", International Journal of Heat and Mass Transfer, 85, 206–220, 2015.

[24] Z. Deng, X. Liu, Ch. Zhang, Y. Huang, Y. Chen, "Melting behaviors of PCM in porous metal foam characterized by fractal geometry", International Journal of Heat and Mass Transfer, 113, 1031–1042, 2017.

[25] M. Esapour, A. Hamzehnezhad, A.A Rabienataj Darzi, M. Jourabian, "Melting and solidification of PCM embedded in porous metal foam in horizontal multi-tube heat storage system", Energy Conversion and Management, 171, 398–410, 2018.

[26] M. Jourabian, A.A Rabienataj Darzi, D. Toghraie and O.A Akbari, "Melting process in porous media around two hot cylinders, Numerical study using the lattice Boltzmann method", Physica A, 509, 316–335 (2018).

[27] Lei Wan, "Numerical investigation of directional solidification processes using a volume averaging technique. Thesis, Cornell University, January (2003).

[28] A.D Brent, VR Voller, KJ Reid, "Enthalpy-porosity technique for modelling convection -diffusion phase change application to the melting of pure metal", Num Heat transfer, 13,297-318, 1988.

[29] B.R Baliga, S.V Patankar, "A new finite-element formulation for convection-diffusion problems", Numerical Heat Transfer, 3, 393-409, 1980.

[30] R. Bennacer, A. Tobbal, H. Béji, "Convection naturelle thermosolutale dans une cavité poreuse anisotrope : formulation de Darcy-Brinkman", Revue. Energy. Renouvelable., 5, 1-21, 2002.

[31] G.Lauriat V. Prasad, "Natural convection in a vertical porous cavity: a numerical study for brinkman-extended Darcy formulation". J. Heat Transfer, 109, 688-696, 1987.

[32] C. Gau, R. Viskanta, "Melting and solidification of a pure metal on a vertical wall", Journal of heat Transfer, 8,174-181, 1986.

[33] J.M. Khodadadi, S.F. Hosseinizadeh, "Nanoparticle-enhanced phase change materials (NEPCM) with great potential for improved thermal energy storage", Int. Commun. Heat Mass Transfer, 34, 534–543, 2007.

[34] S.M. Manar, Al-Jethelah, S. Humaira Tasnim, S. Mahmud, A. Dutta, "Melting of nano-phase change material inside a porous enclosure", International Journal of Heat and Mass Transfer, 102, 773–787, 2016.

[35] M. Mbaye, E. Bilgen, "Phase change process by natural convection-diffusion in rectangular enclosure", Heat and Mass Transfer, 37, 35-42, 2001.

[36] Y. Zhu, B. Huang, J. Wu, "Optimization of filler distribution for organic phase change material composites: Numerical investigation and entropy analysis", Applied Energy, 132, 543-550, 2014.